

Fast Dynamical Evolution of Hadron Resonance Gas via Hagedorn States

M. Beitel,¹ C. Greiner,¹ and H. Stoecker^{1,2,3}

¹*Institut für Theoretische Physik, Goethe-Universität Frankfurt am Main,
Max-von-Laue-Str. 1, D-60438 Frankfurt am Main, Germany*

²*GSI Helmholtzzentrum für Schwerionenforschung GmbH, Planckstraße 1, D-64291 Darmstadt, Germany*

³*Frankfurt Institute for Advanced Studies, Ruth-Moufang-Str. 1, D-60438 Frankfurt am Main, Germany*

Hagedorn states are the key to understand how all hadrons observed in high energy heavy ion collisions seem to reach thermal equilibrium so quickly. An assembly of Hagedorn states is formed in elementary hadronic or heavy ion collisions at hadronization. Microscopic simulations within the transport model UrQMD allow to study the time evolution of such a pure non-equilibrated Hagedorn state gas towards a thermally equilibrated Hadron Resonance Gas by using dynamics, which unlike strings, fully respect detailed balance. Propagation, repopulation, rescatterings and decays of Hagedorn states provide the yields of all hadrons up to a mass of $m = 2.5$ GeV. Ratios of feed down corrected hadron multiplicities are compared to corresponding experimental data from the ALICE collaboration at LHC. The quick thermalization within $t = 1 - 2$ fm/c of the emerging Hadron Resonance Gas exposes Hagedorn states as a tool to understand hadronization.

Before the emergence of QCD as the theory of strong interactions physicists already developed several models and ideas to describe observables in connection with high energetic particle collisions of several types. A prominent phenomenological model is the Statistical Bootstrap Model (SBM) emerging from first applications of statistical means [1–3]. Especially in (ultra-) relativistic heavy ion collisions thermal models [4, 5] seem to show an excellent description of various hadronic particle multiplicities by choosing a temperature, volume and chemical potentials. In this paper we provide a microscopic explanation for the validity of the thermal model and the very fast equilibration at hadronization. In our approach the system temperature equals the Hagedorn temperature.

The Hagedorn temperature T_H is the highest temperature that systems of hadronic particles with an exponentially growing spectrum of (mass) states can have, beyond which the partition function diverges [1]. Beyond T_H deconfinement will start, and, depending on the undersaturation of quarks in the matter [6] a Yang Mills plasma or a 2+1 flavour Quark Gluon Plasma (QGP) will form. T_H in the present approach is identified with the critical temperature T_c . The Hagedorn states (HS) within the SBM are the presently not yet discovered heavy “missing hadron states” which can be attributed to the exponential part of the Hagedorn spectrum and which are most abundant in the vicinity of T_H . In [7] HS being created in multiparticle collisions are proposed to serve as a tool for a microscopic description of the phase transition from HRG to QGP. The HS can have any quantum number combination compatible with their mass. This property of HS was applied in [8–10] in order to understand why (multi-) strange (anti-) hyperons at the Relativistic Heavy Ion Collider (RHIC) chemically equilibrate much faster than the typical life time of a fireball (~ 10 fm/c). In the vicinity of T_H the most abundant mesons, i.e. pions and kaons, do ‘cluster’ to Hagedorn states which in turn can decay into several kinds of hy-

perons. Via a coupled set of rate equations, one for each species, the chemical equilibration times for p, K, Λ are of order $t \sim 1 - 2$ fm/c. The inclusion of Hagedorn spectra in the partition functions of the HRG provides a lowering of the speed of sound, c_s , at the phase transition and a significant decrease of the shear viscosity to entropy ratio η/s [11, 12]. This results are in good agreement with corresponding lattice calculations [13–15]. The general impact of HS on the occurrence of various phases from HRG to deconfined partonic matter was also studied in various MIT bag model descriptions [16–22]. There the Hagedorn spectrum $\rho(m)$ with

$$\rho(m) = f(m) \exp\left(\frac{m}{T_H}\right) \quad (1)$$

is applied, where the pre-function $f(m)$ mimics the low-mass part of the Hagedorn spectrum.

To describe the hadronization of jets in e^+e^- annihilation events the concept of color strings [23] was applied. Here the basic idea is that partons tend to cluster in color singlet states from the very beginning of the generated event. These clusters decay to smaller clusters until some cut-off scale is reached and hadrons are formed [24, 25]. In the framework of RQMD multi-particle collisions and decays were considered as particle clusters for which separable interactions have to exist [26]. A statistical approach [27] considers the hadronization of quark matter droplets to hadrons within the microcanonical ensemble. According to a n -body phase space these quark matter droplets decay via Markov chains into various hadron configurations. A further statistical treatment of HS was performed in Ref. [28] using a simplistic description of the Hagedorn spectrum. The authors regarded one single massive ($m \sim 100$ GeV) initial resonance which consecutively cascades down via decay chains until only stable hadrons as protons, neutrons, pions etc. are left. The various

terms like 'clusters', 'quark matter droplets', 'massive resonances' or 'bags' could be identified with possible Hagedorn states.

Following our recent approach [29] we here implement for the first time Hagedorn states in microscopical dynamical box simulations: In contrast to a non-covariant bootstrap equation [30, 31] we have employed a covariant one

$$\tau_{\vec{C}}(m) = \frac{R^3}{3\pi m} \sum_{\vec{C}_1, \vec{C}_2} \int_{m_1^0}^m dm_1 \int_{m_2^0}^{m-m_1} dm_2 \tau_{\vec{C}_1}(m_1) m_1 \quad (2)$$

$$\times \tau_{\vec{C}_2}(m_2) m_2 p_{cm}(m, m_1, m_2) \delta_{\vec{C}, \vec{C}_1 + \vec{C}_2}^{(3)},$$

where $\tau_{\vec{C}}(m)$ denotes the mass density of Hagedorn states with charge $\vec{C} = (B, S, Q)$ and mass m , where B is the baryon number, S the strangeness and Q the electric charge. The terms $\tau_{\vec{C}_1}$ and $\tau_{\vec{C}_2}$ stand for spectra of both constituents which make up spherical HS with radius R whose density is described by $\tau_{\vec{C}}(m)$. In the rest frame of created HS, p_{cm} denotes the momenta of the decay products and ensures strict energy-momentum conservation. Exact charge conservation is applied too. This highly non-linear integral equation of Volterra type is solved numerically. The initial input for $\tau_{\vec{C}_{1,2}}$ are spectral functions of the hadronic transport model UrQMD (Ultrarelativistic Quantum Molecular Dynamics) [32] consisting of 55 baryons and 32 mesons. Inserting the hadronic spectral functions into the r.h.s. of Eq. 2 results in first HS consisting of two hadrons only. In the subsequent steps, these created HS serve as constituents of next heavier HS, which now may consist of one HS and one hadron or of two lighter HS. This means that every Hagedorn spectrum on the l.h.s. sooner or later will appear as constituent on the r.h.s. of Eq. 2 to create next heavy HS. The upper Hagedorn spectrum mass m is increased by $\Delta m = 0.01 \text{ GeV}$ until a final value of $m = 8.6 \text{ GeV}$ is reached due to computational limitations. Numerical results of Eq. 2 are provided in [29]. We find that the Hagedorn temperature rises when R gets smaller and is very weakly dependent on charges \vec{C} . In addition with the Hagedorn spectrum we were able to derive an expression for HS total decay width Γ

$$\Gamma_{\vec{C}}(m) = \frac{\sigma}{2\pi^2 \tau_{\vec{C}}(m)} \sum_{\vec{C}_1, \vec{C}_2} \int_{m_1^0}^m dm_1 \int_{m_2^0}^{m-m_1} dm_2 \tau_{\vec{C}_1}(m_1) \tau_{\vec{C}_2}(m_2)$$

$$\times p_{cm}(m, m_1, m_2)^2 \delta_{\vec{C}, \vec{C}_1 + \vec{C}_2}^{(3)}. \quad (3)$$

To compute $\Gamma_{\vec{C}}$ we applied the principle of detailed balance between binary collisions to create HS and their decays into two particles, i. e. $2 \rightarrow 1$ and $1 \rightarrow 2$ only. The limitation to $2 \leftrightarrow 1$ processes is necessary when implementing HS into a customary

cascade-type transport model which is based on a geometrical interpretation of cross sections as it is now implemented in UrQMD. The total decay width is expressed in terms of HS creation cross section σ which are in the range $\Gamma \approx 0.4 - 3.5 \text{ GeV}$. Various results can be found in [29]. There are some light HS whose total decay width exceeds the mass. Their total yield is less than 15%, so we decided to ignore this small effect.

The HS with mass m , quantum numbers \vec{C} , total decay width $\Gamma_{\vec{C}}$ and the various branching ratios \mathcal{BR} have, in the present work, been implemented fully into the UrQMD model. The evolution from nonequilibrated initial HS gas through detailed balance between HS creations and HS decays to equilibrated HRG is simulated in a $10 * 10 * 10 \text{ fm}^3$ cubic box with reflecting walls. Each simulation is done at an energy density between $\epsilon = 0.3 - 2.0 \text{ GeV/fm}^3$ in steps of $\Delta\epsilon = 0.1 \text{ GeV/fm}^3$. The quantum numbers of all initial heavy HS in the box are assumed to have $\vec{C} = (0, 0, 0)$ to simulate an uncharged gas. The time evolution will therefore produce all charges \vec{C} only by the decays of HS into charged hadrons and lighter HS, as is the case in ultrarelativistic heavy ion collisions at RHIC and at the LHC, where all the net charges at midrapidity are close to zero, e. g. a net baryon density of $\rho_B \approx 0$ has been measured. Thus the initial ensemble of (heavy) HS creates dynamically all kinds of (light) hadrons until chemical equilibrium between HS and hadrons is achieved. As a more conventional alternate conceptual point of view consider the following picture of hadronization: In an (ultra-) relativistic collision of two heavy ions a large QGP drop is being created. This drop expands, cools and decays into smaller droplets/HS close to the transition temperature $T_H \approx T_c$. The HS propagate, collide with each other and with hadrons, until they decay. Among the decay products of the HS at first hadrons will appear quasi instantly. The hadrons and the HS may create new HS or hadrons, which then can go on to collide elastically or inelastically with each other. As long as the system stays at a high temperature $T \approx T_H$ the dynamical interplay between hadrons and HS will drive both into thermal and chemical equilibrium. To examine this process we distribute initial HS uniformly in momentum and configuration space and demand:

$$E = \sum_{i=1}^{N_0} E_i, \quad \vec{p} = \sum_{i=1}^{N_0} \vec{p}_i = 0 \quad (4)$$

The initial number of HS is set to $N_0 = 200$. Each run lasts until $t = 20 \text{ fm}/c$ and all results are averaged over 1200 runs.

Fig. 1 shows the final mass distribution of all HS which arises when a system with exponential growth of mass states is subjected to the Boltzmann distribution. The equilibrated mass distribution of HS shown in Fig. 1 re-

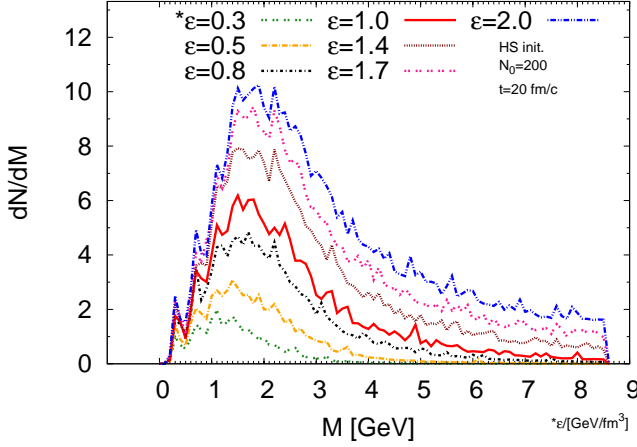


FIG. 1: Mass distribution of HS in thermal equilibrium ($t = 20 \text{ fm}/c$) for energy densities in the range $\epsilon = 0.3 - 2.0 \text{ GeV}/\text{fm}^3$.

sults from the convolution of the Hagedorn spectrum $\tau \sim \exp(m/T_H)$ and the Boltzmann distribution $f(E) \sim \exp(-E/T)$. Observe that for higher energy densities more HS with higher masses are formed. The impact of HS on the system's total particle number, energy and mass after $t = 5 \text{ fm}/c$ is shown in Fig. 2. At the largest energy density, $\epsilon = 2.0 \text{ GeV}/\text{fm}^3$, already every fourth particle is a HS and more than $\sim 60\%$ of the total energy and $\sim 70\%$ of the total mass are occur by HS. All results are in full accordance to the SBM: HS appear most abundantly at T_H , which is reached when $\epsilon \rightarrow \infty$. We also observe that with increasing energy density more and more of the available total energy is converted into (massive) HS rather than being distributed over the kinetic degrees of freedom. The latter result is backed by the dependence of hadrons' Boltzmann slopes T on ϵ as shown in the lower part of Fig. 2. Increasing energy density ϵ causes the temperature T of all hadrons to converge to the Hagedorn temperature T_H . This result contradicts the usual HRG thermodynamics, where the temperature grows with the energy density beyond any limit. Our result manifests the SBM statement

$$\lim_{\epsilon \rightarrow \infty} T = T_H. \quad (5)$$

Note that decay chains of a single massive HS already show slopes with a Hagedorn temperature [29], - a consistent picture.

Observe the very fast thermalization time $t = 1 - 2 \text{ fm}/c$, where hadrons, hadron resonances and HS interact rapidly, changing energy and quantum numbers. Fig. 3 shows the time evolution of pions, kaons, protons and lambdas as 'direct' decay hadrons and feed down of hadron resonances and of HS. The later feed down corresponds to (potential) hadronic particles 'stored' in the existing HS as calculated via

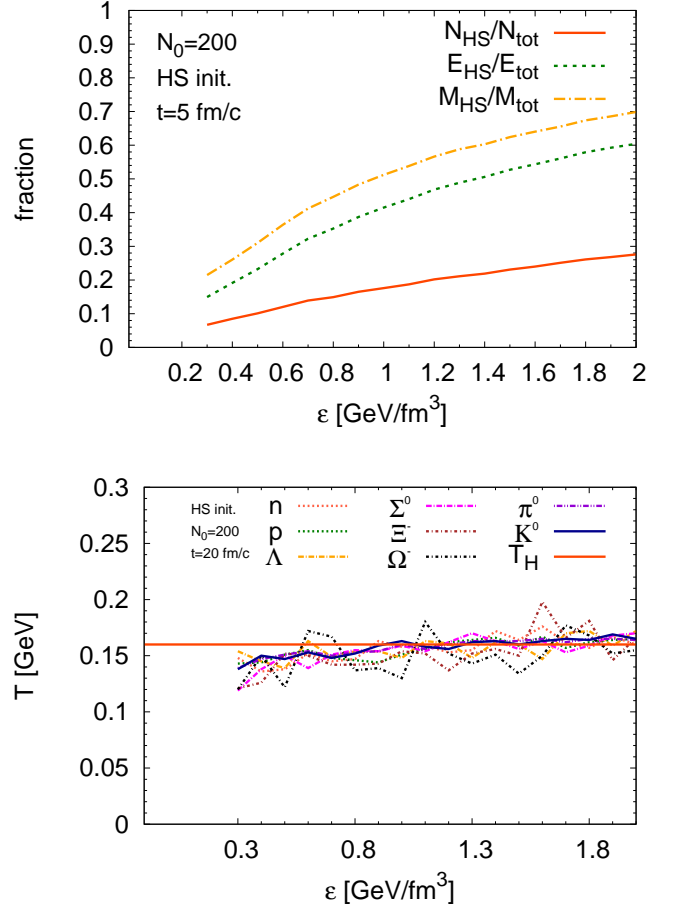


FIG. 2: Fraction (top) of total multiplicities, energy and mass occupied by HS in thermal equilibrium ($t \geq 5 \text{ fm}/c$) as function of energy density. Boltzmann slopes (temperatures) of hadrons (bottom) as function of energy density in thermal equilibrium ($t = 20 \text{ fm}/c$). Red solid line denotes the Hagedorn temperature T_H .

their decay chains as discussed in [29]. The very fast thermalization in our simulations of $t \leq 2 \text{ fm}/c$ is now obtained from the initial decaying HS in the system. The upper figure shows that the number of HS drops down within $t = 1 \text{ fm}/c$ and then saturates. The emerging hadrons and hadronic resonances are build up during by these decays and by the subsequent regenerations of HS on such short time scale (lower figure). The sum of the yield hadrons stemming from feed down of the HS and of hadronic resonances (shown in the lower figure) accounts for the total stable particle yields in the upper figure. Within $t = 1 \text{ fm}/c$ more than a half of the initial HS has decayed into hadrons reaching a stationary value at $t = 1 - 2 \text{ fm}/c$ and a further moderate saturation. The very fast chemical equilibration occurs by means of decays, recreation and rescatterings of HS in such a dense environment. This is in contrast to standard hadronic transport approaches of [33, 34].

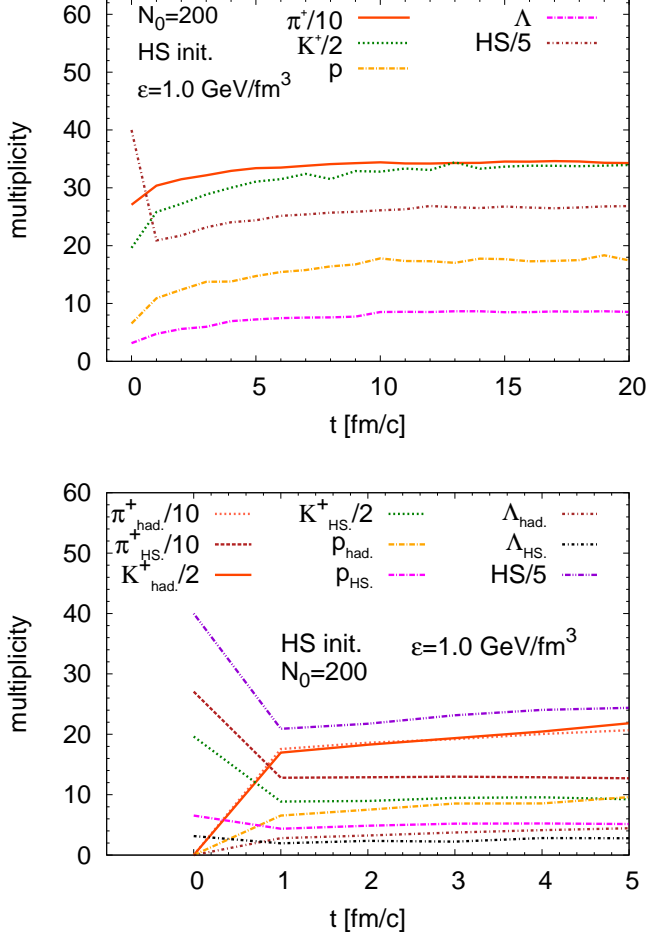


FIG. 3: Time evolution of total (feed down corrected) multiplicities (top) of π^+ , K^+ , p and Λ^0 at energy density $\epsilon = 1.0 \text{ GeV/fm}^3$. Time evolution (bottom) of first 5 fm/c of direct multiplicities plus feed down contributions from resonance decay (had.) and from HS decays (HS.) for same hadrons as mentioned above. In case of HS direct multiplicities were considered.

Fig. 4 shows that in chemical equilibrium total multiplicities rise nearly linear with energy density in the evolving system originating from the initial assembly of HS. The yields are determined predominantly by the particle's masses. HS exhibit the steepest slope as demanded by SBM. Tab. I confronts the calculated hadron multiplicity ratios at different energy densities with corresponding experimental values as obtained by the ALICE collaboration at the LHC. To demonstrate that a real thermal (chemical+kinetic) equilibrium is reached we compare in Fig. 5 simulated hadron multiplicities at $\epsilon = 1.0 \text{ GeV/fm}^3$ with multiplicities provided by a standard HRG thermal model. A temperature of $T \sim 0.154 \text{ GeV}$ is assumed in the thermal model and for $\epsilon = 1.0 \text{ GeV/fm}^3$ in the full evolution as depicted in Fig. 2. The perfect agreement supports that our results

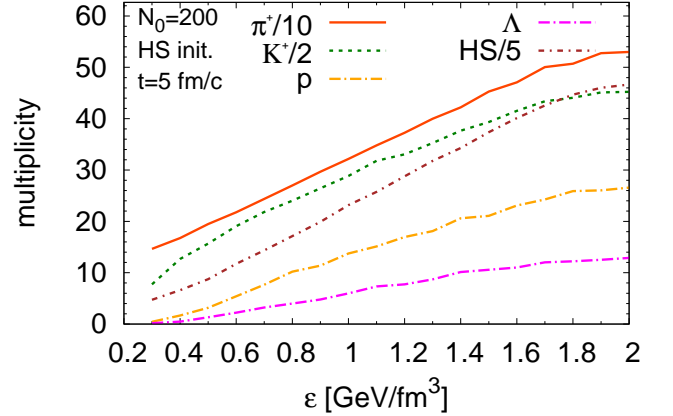


FIG. 4: Total multiplicity dependence on energy density of π^+ , K^+ , p and Λ^0 close to chemical equilibrium ($t = 5 \text{ fm/c}$). In case of HS dynamical multiplicities were considered.

	p-p	Pb-Pb	0.3	0.8	1.0	2.0
K^-/π^-	0.123(14)	0.149(16)	0.192	0.197	0.193	0.185
\bar{p}/π^-	0.053(6)	0.045(5)	0.015	0.049	0.052	0.060
Λ/π^-	0.032(4)	0.036(5)	0.007	0.022	0.024	0.029
Λ/\bar{p}	0.608(88)	0.78(12)	0.475	0.456	0.469	0.499
$\Xi^-/\pi^- * 10^3$	3.000(1)	5.000(6)	1.565	6.492	5.769	7.106
$\Omega^-/\pi^- * 10^3$	-	0.87(17)	0.137	0.815	0.823	0.994

TABLE I: Comparison of particle multiplicity ratios from theory vs. p-p at $\sqrt{s_{NN}} = 0.9 \text{ TeV}$ [35] and Pb-Pb at $\sqrt{s_{NN}} = 2.76 \text{ TeV}$ [36–38], both from ALICE at LHC. Calculated values are listed for some energy densities in the range $\epsilon = 0.3 - 2.0 \text{ GeV/fm}^3$. Numbers in brackets denote the error in the last digits of the experimental multiplicity ratios. The statistical error is less than 25% for strange baryons.

thermally equilibrated.

In summary, it was shown that a system of HS, e. g. as emerging of large QGP drops created in heavy ion collisions gives a new insight how hadronization can take place. Starting in non-equilibrium dynamical decay and (re-) creation of HS provide on a very short time scale of $t = 1 - 2 \text{ fm/c}$ all hadrons of the HRG as advocated over the years in [4, 5]. Potential decays of HS might also explain the finding of $e^- - e^+$ [39] and $p - \bar{p}$ [40] within a thermal model analysis. The implementation in microscopic transport models of full heavy ion collisions sets a new venue at future investigations, also for finite net baryon densities at NICA facilities in Dubna and CBM experiments at the FAIR facility which is build adjacent to the GSI in Darmstadt. Multibaryonic and multistrange HS can serve as an energy reservoir for production of rare hadronic particles. The implications of HS on the shear viscosity and on the net baryon number fluctuations in

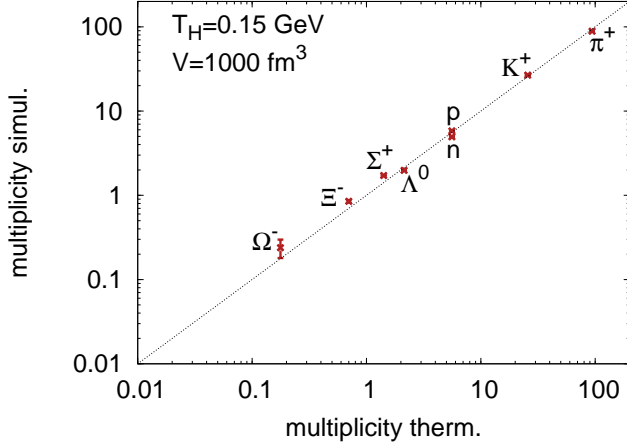


FIG. 5: Hadronic multiplicities from dynamical box simulation (ordinate) for $\epsilon = 1.0 \text{ GeV/fm}^3$ ($T \approx 0.154 \text{ GeV}$) at $t = 20 \text{ fm/c}$ and corresponding thermal model (abscissa) for $T = 0.154 \text{ GeV}$ and $V = 1000 \text{ fm}^3$. Statistical error in simulations is for Ω^- roughly 25% and for others less than 5%.

dense hadronic matter has to be studied in the future.

We thank K. Gallmeister for critical discussions. This work was supported by the Bundesministerium für Bildung und Forschung (BMBF), the HGS-HIRE for FAIR and GSI, the Helmholtz International Center for FAIR within the framework of the LOEWE program launched by the State of Hesse. Numerical computations have been performed at the Center for Scientific Computing (CSC) at the Goethe Universität Frankfurt.

[1] R. Hagedorn, *Nuovo Cim. Suppl.* **3**, 147 (1965).
[2] R. Hagedorn and J. Ranft, *Nuovo Cim. Suppl.* **6**, 169 (1968).
[3] R. Hagedorn, *Nuovo Cim. Suppl.* **6**, 311 (1968).
[4] P. Braun-Munzinger, D. Magestro, K. Redlich, and J. Stachel, *Phys. Lett. B* **518**, 41 (2001).
[5] A. Andronic, P. Braun-Munzinger, K. Redlich, and J. Stachel, *J. Phys. G* **38**, 124081 (2011), 1106.6321.
[6] H. Stoecker et al. (2015), 1509.00160.
[7] C. Greiner, P. Koch-Steinheimer, F. M. Liu, I. A. Shovkovy, and H. Stoecker, *J. Phys. G* **31**, S725 (2005).
[8] J. Noronha-Hostler, C. Greiner, and I. A. Shovkovy, *Phys. Rev. Lett.* **100**, 252301 (2008).
[9] J. Noronha-Hostler, C. Greiner, and I. Shovkovy, *J. Phys. G* **37**, 094017 (2010).
[10] J. Noronha-Hostler, M. Beitel, C. Greiner, and

I. Shovkovy, *Phys. Rev. C* **81**, 054909 (2010).
[11] J. Noronha-Hostler, J. Noronha, and C. Greiner, *Phys. Rev. Lett.* **103**, 172302 (2009).
[12] J. Noronha-Hostler, J. Noronha, and C. Greiner, *Phys. Rev. C* **86**, 024913 (2012).
[13] A. Majumder and B. Muller, *Phys. Rev. Lett.* **105**, 252002 (2010).
[14] A. Jakovac, *Phys. Rev. D* **88**, 065012 (2013).
[15] K. Itakura, O. Morimatsu, and H. Otomo, *J. Phys. G* **35**, 104149 (2008).
[16] L. Moretto, K. Bugaev, J. Elliott, and L. Phair, *Europhys. Lett.* **76**, 402 (2006).
[17] I. Zakout, C. Greiner, and J. Schaffner-Bielich, *Nucl. Phys. A* **781**, 150 (2007).
[18] I. Zakout and C. Greiner, *Phys. Rev. C* **78**, 034916 (2008).
[19] L. Ferroni and V. Koch, *Phys. Rev. C* **79**, 034905 (2009).
[20] K. Bugaev, V. Petrov, and G. Zinovjev, *Phys. Rev. C* **79**, 054913 (2009).
[21] A. Ivanytskyi, K. Bugaev, A. Sorin, and G. Zinovjev, *Phys. Rev. E* **86**, 061107 (2012).
[22] V. Vovchenko and H. Stoecker (2015), 1512.08046.
[23] B. Andersson, G. Gustafson, G. Ingelman, and T. Sjöstrand, *Phys. Rept.* **97**, 31 (1983).
[24] B. Webber, *Nucl. Phys. B* **238**, 492 (1984).
[25] G. Marchesini, B. Webber, G. Abbiendi, I. Knowles, M. Seymour, et al., *Comput. Phys. Commun.* **67**, 465 (1992).
[26] H. Sorge, H. Stoecker, and W. Greiner, *Annals Phys.* **192**, 266 (1989).
[27] K. Werner and J. Aichelin, *Phys. Rev. C* **52**, 1584 (1995).
[28] S. Pal and P. Danielewicz, *Phys. Lett. B* **627**, 55 (2005).
[29] M. Beitel, K. Gallmeister, and C. Greiner, *Phys. Rev. C* **90**, 045203 (2014), 1402.1458.
[30] S. C. Frautschi, *Phys. Rev. D* **3**, 2821 (1971).
[31] C. Hamer and S. C. Frautschi, *Phys. Rev. D* **4**, 2125 (1971).
[32] S. Bass, M. Belkacem, M. Bleicher, M. Brandstetter, L. Bravina, et al., *Prog. Part. Nucl. Phys.* **41**, 255 (1998).
[33] M. Belkacem, M. Brandstetter, S. Bass, M. Bleicher, L. Bravina, et al., *Phys. Rev. C* **58**, 1727 (1998), nucl-th/9804058.
[34] E. Bratkovskaya, W. Cassing, C. Greiner, M. Effenberger, U. Mosel, et al., *Nucl. Phys. A* **681**, 84 (2001), nucl-th/0007019.
[35] K. Aamodt et al. (ALICE Collaboration), *Eur. Phys. J. C* **71**, 1594 (2011).
[36] B. Abelev et al. (ALICE Collaboration), *Phys. Rev. C* **88**, 044910 (2013).
[37] B. B. Abelev et al. (ALICE Collaboration), *Phys. Rev. Lett.* **111**, 222301 (2013).
[38] B. B. Abelev et al. (ALICE Collaboration), *Phys. Lett. B* **728**, 216 (2014).
[39] F. Becattini, *Z. Phys. C* **69**, 485 (1996).
[40] F. Becattini and U. W. Heinz, *Z. Phys. C* **76**, 269 (1997).